Zeitschrift für Kristallographie 211, 440–448

The crystal structure of a blatterite mineral, $Mg_{1.33}Mn_{1.44}Fe_{0.05}Sb_{0.17}O_2BO_3$, a combined single crystal X-ray and HREM study

J.-O. Bovin*, A. Carlsson, R. Sjövall, R. Thomasson

Lund University, Chemical Center, National Center for HREM, P.O. Box 124, S-22100 Lund, Sweden

R. Norrestam

University of Stockholm, Arrhenius Laboratory, Department of Structural Chemistry, S-10691 Stockholm, Sweden

and I. Søtofte

The Technical University of Denmark, Chemistry Department B, DTH 301, Structural Chemistry Group, DK-2800 Lyngby, Denmark

Dedicated to Professor Georg von Schnering on the occasion of his 65th birthday

Received July 24, 1989; accepted in final form December 8, 1995

Crystal structure / X-ray diffraction / Cation ordering / HREM / Micro EDX analysis

Abstract. The borate mineral $Mg_{1.33}Mn_{1.44}Fe_{0.05}Sb_{0.17}O_2BO_3$ from the Mossgruvan mine, Nordmark, Värmland, Sweden, has been studied by a combination of single crystal X-ray diffraction and electron microscopy (HREM, EELS and EDX) techniques. The HREM investigations showed that the structure belongs to the pinakiolite family, whose other members with increasing complexity are, e.g. pinakiolite, ludwigite, orthopinakiolite, takéuchiite and blatterite. The space group is orthorhombic, *Pnnm* (No. 58), $a = 37.384(11)$ Å, $b = 12.568(3)$ Å, $c = 6.200(2)$ Å; $Z = 32$. The structural model, for which the initial coordinates could be deduced from the HREM images, has been refined versus the 2280 most significant X-ray reflection intensities with $\sin\theta/\lambda \leq 0.70$ Å^{-1} to R-value of 0.056.

As for many other members of the pinakiolite family some cation positions are disordered. The disorder is obviously related to the structural effects caused by the distorted oxygen coordination octahedra around the Mn^{3+} ions. As revealed by HREM, some blatterite crystals contain extended planar defects that can be explained as due to irregular repeat distances between the twin planes in the [100] direction.

Introduction

The mineral blatterite belongs to the pinakiolite group of minerals. It was given its mineral name by Raade, Mladek, Din, Criddle and Stanley (1988). Although the chemical composition of their specimen, $Mg_{0.79}Mn_{1.90}Fe_{0.11}Sb_{0.19}O_2BO_3$, differs from that found in the present study, HREM studies (Bovin, Barry, Thomasson, Norrestam, Fälth, 1986 and Raade et al., 1988) verified that the specimen was a new structural member of the family. The existence of this member was pointed out earlier by Dunn, Peacor, Simmons and Newbury (1983), who gave the composition $Mg_{1.59}Mn_{1.54}Fe_{0.11}Al_{0.01}Sb_{0.15}O_2BO_3$, but its structure was believed to be very disordered in the [100] direction. Preliminary investigations (Bovin et al., 1986) of the present mineral showed it to be rather well ordered.

The pinakiolite family consists of at least twelve known members with the general formula $M_3O_2BO_3$. The metal ions, M, can be divalent as Mg^{2+}, Mn^{2+}, Fe^{2+}, Ni^{2+} and/or trivalent as Mn^{3+}, Fe^{3+}, Al^{3+} and also tetra- and pentavalent as Sn^{4+}, Ti^{4+} or Sb^{5+}. With the concept of chemical twinning (Andersson, Hyde, 1974), the structures of the different members of the family can be considered as built up by twinning of the parent structure of pinakiolite (or hulsite) as presented by Takéuchi (1978) and by Bovin, O'Keeffe and O'Keefe (1981). The metal ions are octahedrally coordinated by oxygen ions and the octahedra are linked together by corner- and edge-sharing to form flat walls, **F** walls, and zig-zag walls. With the notation of Takéuchi (1978) the central columns of octahedra through the zig-zag walls are called **C** walls.

Most of the members of the family are possible to synthesize and several, not known as minerals, have been prepared, e.g. $Co_3O_2BO_3$ (Norrestam, Nielsen, Søtofte, Thorup, 1988). As the structure type is able to host i.a. ions of different valences of the same element, members of the family are potential catalysts. Preliminary tests of some ludwigites have already shown that they have some catalytic activity in the total oxidation of hydro-carbons.

* Correspondence author

The crystal structure of blatterite is of interest as it is the most complex member of the pinakiolite family hitherto known in crystalline form. Furthermore, structural investigations of two other members, takéuchiite (Norrestam, Bovin, 1987) and a new antimony rich variant of pinakiolite (Norrestam, Hansen, 1988) have shown that the structural implications of the Jahn-Teller effect for the Mn^{3+} ions cause extended positional disorder of the metal (not Mn^{3+}) ions in every second layer of octahedra in the C walls. The aim of this investigation is thus also to study this apparently general feature of the family members containing Mn^{3+} further.

Experimental

The specimen of blatterite investigated in the present study, was found 1976 in the dumps at the Mossgruvan mine, Nordmark, Värmland, Sweden, by James Anstett. The mineral occurs as black prismatic striated crystals, oriented in bands, associated mainly with hausmannite and calcite. These species were verified by powder diffraction techniques. The holotype specimen is deposited at the Swedish Museum of National History (specimen No. NRM 890001).

Electron microscopy studies

Black prismatic crystals were selected for studies in a scanning electron microscope, JSM-840A, equipped with a LINK AN10000 energy dispersive X-ray (EDX) analysing system. The EDX spectra were collected for several crystals and at many regions (excited area approximately $4 \cdot 10^{-6}$ m in diameter) on each crystal. A typical EDX spectrum from the crystal used for the X-ray investigation is shown in Fig. 1a. The spectra were evaluated with the computer program ZAF-4/FLS (Statham, 1977), using standard spectra collected from pure oxides of the present metals. The mean value of several crystals, six spectra from each crystal, gave the chemical composition $Mg_{1.33(2)}Mn_{1.44(2)}Fe_{0.05(1)}Sb_{0.17(1)}O_2BO_3$. The estimated standard deviations (e.s.d.'s) take into account spatial as well as methodical variations. In order to verify the presence of the light elements, an electron energy loss spectrum (EELS) was recorded (Fig. 1b) with a Gatan 666 parallel EELS using a JEM-2000FX operated at 200 kV. The analyses are in good accordance with those calculated from the metal ion occupancies found by the X-ray diffraction study, but differ considerably from those given by Raade et al. (1988). No crystal with a composition similar to that proposed by Raade et al. was found in the present specimen. It is most likely, that the crystals investigated by Raade et al. are from another part of the Nordmark ore field and it can be concluded that there are different compositional variants of the blatterite mineral.

Several crystals of the mineral were ground in acetone and deposited on a holey carbon film supported on a copper grid. The crystals were first investigated for unit cell dimensions and structure type by means of high resolution electron microscopy (HREM). The microscopes used were JEM-200CX and Philips EM430, both with a structural resolution power of 2.3 Å. Selected

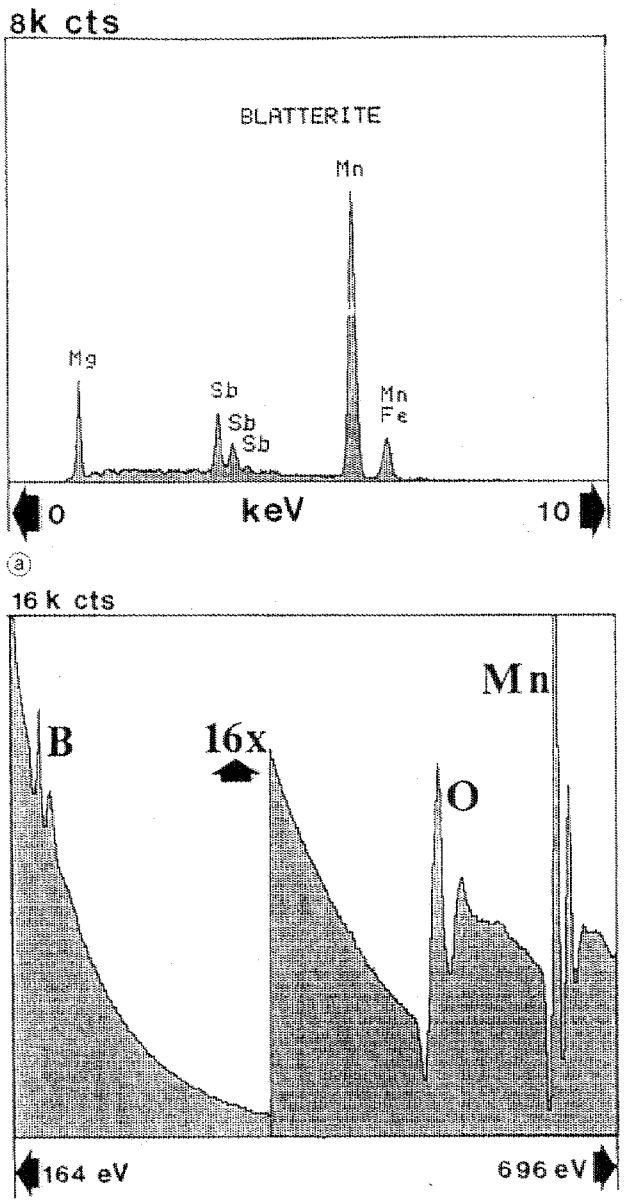

Fig. 1. (a) Typical energy dispersive X-ray (EDX) spectrum of the blatterite crystal investigated by X-ray single crystal diffraction. The spectrum was recorded at 20 kV in a scanning microscope. (b) Second difference electron energy loss spectrum (EELS) from a blatterite crystal showing the K edges for B and O, and the $L_{2,3}$ edges of Mn. There is a 16× gain shift in the middle of the spectrum.

area electron diffraction patterns recorded along [001] (Fig. 2a) showed that all the crystals belonged to the new -8t8t8t- member (t stands for twin plane) of the pinakiolite family. Direct structural imaging at Scherzer focus (Fig. 2b) confirmed this observation and showed that the structure type was similar to that of the -6t6t6t- member, takéuchiite (Norrestam, Bovin, 1987), of the pinakiolite family. The image in Fig. 2b also shows in profile the structure of one of the dominating surface {010} of the crystals. Computer image simulations indicate that the atoms of the C wall are facing the surface. Some of the

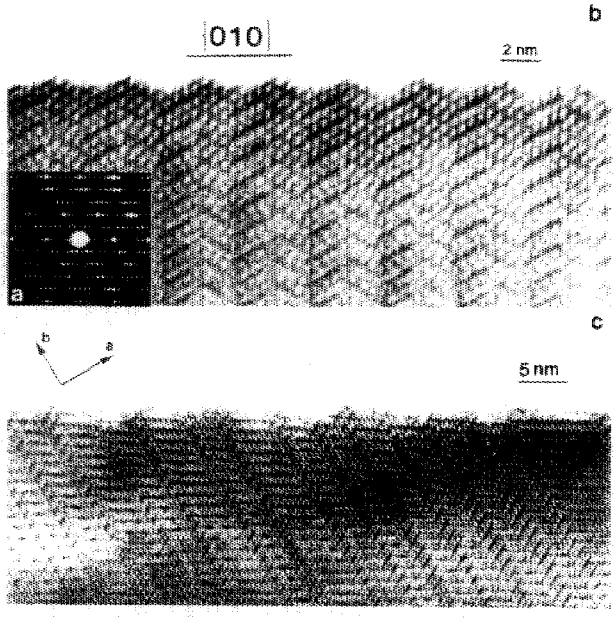

Fig. 2. (a) Selected area diffraction pattern recorded with the beam along [001] of a well ordered crystal fragment of the mineral blatterite. (b) High resolution electron micrograph of a crystal, recorded with a Philips EM430 TEM working at 300 kV. Note, that the {010} surface is imaged in profile, at Scherzer focus, revealing that the atoms of the C walls are mostly facing the surface. (c) TEM electron micrograph of a very disordered (along [100]) crystal. The image was recorded in a JEM 2000CX at 200 kV, with the electron beam parallel to [001].

crystals were very disordered along [100] (Fig. 2c) and such extended planar defects are very common in many members of the family, as shown by HREM (Bovin, O'Keeffe, O'Keefe, 1981). Regarding the twin sequence -8t8t8t-, most of the crystals were well ordered with only scattered sequence mistakes.

Further HREM investigations were performed with a JEM-4000EX operated at 400 kV and capable of performing studies with a structural resolution of 1.6 Å. An image (Fig. 6a) recorded at about 45 nm underfocus was digitized with a CCD camera with 512 × 512 pixels and 256 grey levels. The digitized image was processed and Fourier transformed using the Semper image processing package. The reciprocal lattice was indexed and the lattice parameters determined using the positions of the strongest peaks in the transform. The local background was subtracted, and the amplitudes and phases of the peaks were refined. This refinement is necessary, since the peaks are often spread over several pixels due to inexact sampling. The refined values were used to reconstruct an average image (Fig. 6b). In order to correct for loss in phase information, due to beam and crystal tilt, the image was symmetrized (Misell, 1978) using the two-dimensional space group *pgg* for the [001] projection of the X-ray determined space group, *Pnnm*. Image simulation (Fig. 6d) was performed with the EMS software (Stadelmann, 1987). The parameters used were: spherical aberration constant 1.0 mm, semi-angle of beam convergence 0.5 mrad and focus spread 5 nm.

Table 1. Experimental conditions for the structure determination of blatterite.

Formula (from EDX)	$Mg_{1.33}Mn_{1.44}Fe_{0.05}Sb_{0.17}O_2BO_3$
Crystal shape; Crystal size	Prismatic; 0.04 × 0.08 × 0.19 mm
Formula weight	255.7
Space group (no.); Z	*Pnnm* (58); 32
Unit cell dimensions (293(1) K)	a = 37.384(11) Å, b = 12.568(3) Å, c = 6.200(2) Å
Unit cell volume, V	2913(1) Å^3
Calculated density, D_x	4.18 g cm^{-3}
Radiation; Wavelength, λ	MoK_α; 0.71073 Å
Intensity data collection:	
Maximum sin $(\theta)/\lambda$	0.700 Å^{-1}
Range of h, k and l	0 to 49, 0 to 17 and 0 to 8
Standard reflections	2
Intensity instability	<3%
Number of unique reflections	3670
Number of observed reflections	2280 ($I > 5\sigma(I)$)
Number of refined parameters	217
Absorption correction:	
Linear absorption coefficient	67.0 cm^{-1}
Transmission factor range	0.66 to 0.82
Structure:	
Minimization of	$\sum wA F^2$
Weighting scheme	$[\sigma^2(F) + 0.00005\|F\|^2)^{-1}$
Final R; wR	0.0497; 0.0625
Final ϱ_{min} and ϱ_{max}	−1.9 and 4.2e^-/Å^3

X-ray diffraction studies

The possible space groups *Pnnm* and *Pnn*2 of a selected single crystal was derived from photographic X-ray diffraction studies using de Jong and precession techniques. The space group symmetries agree with those found for other Mn^{3+} containing members of the pinakiolite family (see e.g. Norrestam and Bovin, 1987), which have their c-axis doubled (around 6 Å) compared to the nondistorted members (e.g. Norrestam, Dahl, Bovin, 1989). The deviation from an ideal symmetry leads to an uneven distribution of X-ray diffraction intensities for different values of the l index. Thus, reflections with l odd are generally much weaker than those with l even. In combination with the limited size of the crystals available, this implies limitations on the possibilities of collecting an extensive set of significant X-ray diffraction intensities. The fraction of observable intensities in the present case is 62% (Table 1). The X-ray diffraction data collected with a single crystal diffractometer, Enraf-Nonius CAD4, were corrected for background, Lorentz, polarization and absorption effects. Further details on the experimental conditions are given in Table 1. The centrosymmetrical space group *Pnnm* adopted in this study is supported by the outcome of the structural refinements.

Structure determination and refinement

HREM investigations (Fig. 2) verified that the present crystals belonged to the pinakiolite family. Thus, initial coordinates of the atomic positions for an ideal blatterite structure could be deduced by numerically applying the periodic twinning model (Andersson, Hyde, 1974) on the idealized parent structure of pinakiolite. As mentioned

Table 2. Fractional atomic coordinates ($\times 10^4$) and thermal parameters ($\times 10^4$ Å^2) for blatterite. The scattering factors used for the metal atoms M(1), M(5a), M(5b) and M(14) to M(19) were linear combinations of neutral Mg and Mn, constrained to give metal contents of 100%. The anisotropic temperature factor expression used for the pure Sb positions (M(2) and M(13)) was: $\exp[-2\pi^2((ha^*)^2 U_{11} + \ldots + 2hka^*b^*U_{12})]$.

% Mg	Atom	x	y	z	U_{11}
69(2)	M(1)	0	0	0	51(15)
0[Sb]	M(2)[a]	0	0	1/2	32(5)
100	M(3)	100	4628(11)	0	345(32)
0	M(4)	0	1/2	1/2	62(6)
27(2)	M(5a)	273(2)	4089(5)	0	228(14)
27(2)	M(5b)	525(2)	3992(5)	0	228(14)
0	M(6)	635(1)	3961(2)	1/2	61(4)
0	M(7a)	1042(3)	3648(9)	0	96(8)
0	M(7b)	1271(4)	2825(11)	0	96(8)
0	M(7)	1197(1)	3070(2)	0	96(8)
0	M(8)	1257(1)	2855(2)	1/2	58(4)
0	M(9)	1865(1)	1813(2)	0	162(5)
0	M(10)	1896(1)	1842(2)	1/2	58(4)
0	M(11)	2531(1)	649(2)	0	126(5)
0	M(12)	2524(1)	663(2)	1/2	77(5)
0[Sb]	M(13)[b]	3747(1)	2881(1)	0	39(4)
59(2)	M(14)	3745(1)	2881(3)	1/2	68(10)
63(1)	M(15)	614(1)	1726(2)	2502(4)	85(7)
49(1)	M(16)	1891(1)	4064(1)	2481(4)	85(6)
69(1)	M(17)	3140(1)	4610(2)	2463(5)	82(7)
78(1)	M(18)	3102(1)	1842(2)	2562(5)	77(7)
54(1)	M(19)	4362(1)	1163(2)	2521(3)	92(6)
100	M(20)	4367(1)	3961(2)	2588(5)	17(5)
	O(1)	399(1)	322(5)	2667(12)	60(12)
	O(2)	284(2)	2428(8)	0	65(23)
	O(3)	298(3)	2429(9)	1/2	117(25)
	O(4)	357(2)	4694(5)	2889(11)	65(13)
	O(5)	979(3)	1347(8)	0	103(23)
	O(6)	988(3)	1245(8)	1/2	79(22)
	O(7)	896(2)	3189(5)	2851(11)	85(14)
	O(8)	1540(3)	368(8)	0	89(24)
	O(9)	1549(2)	320(7)	1/2	32(21)
	O(10)	1609(1)	2557(5)	2817(11)	52(12)
	O(11)	1497(3)	4462(8)	0	114(24)
	O(12)	1526(3)	4532(7)	1/2	45(21)
	O(13)	2152(1)	1070(5)	2809(11)	55(13)
	O(14)	2196(3)	3221(8)	0	82(24)
	O(15)	2216(3)	3375(8)	1/2	60(23)
	O(16)	2842(1)	427(5)	2691(12)	59(12)
	O(17)	2756(3)	2260(8)	0	97(22)
	O(18)	2761(3)	2354(8)	1/2	87(23)
	O(19)	2758(2)	4154(8)	0	64(20)
	O(20)	2791(2)	4234(8)	1/2	83(21)
	O(21)	3488(3)	1419(8)	0	64(20)
	O(22)	3497(3)	1385(8)	1/2	94(22)
	O(23)	3413(2)	3223(4)	2335(12)	60(13)
	O(24)	4040(3)	461(8)	0	82(25)
	O(25)	4053(3)	447(9)	1/2	143(29)
	O(26)	4086(1)	2573(5)	2340(11)	54(12)
	O(27)	4001(2)	4352(8)	0	59(19)
	O(28)	4016(2)	4429(8)	1/2	81(22)
	O(29)	4738(3)	1637(8)	0	108(26)
	O(30)	4736(3)	1614(8)	1/2	108(25)
	O(31)	4750(2)	3548(8)	0	64(21)
	O(32)	4720(2)	3507(8)	1/2	62(21)
	B(1)	1177(4)	403(12)	0	70(8)
	B(2)	1183(4)	356(12)	1/2	70(8)
	B(3)	2560(4)	3210(13)	0	70(8)
	B(4)	2593(4)	3302(13)	1/2	70(8)
	B(5)	3685(4)	445(12)	0	70(8)
	B(6)	3676(4)	455(12)	1/2	70(8)
	B(7)	4926(4)	2544(13)	0	70(8)
	B(8)	4910(4)	2581(13)	1/2	70(8)

[a] U_{22} 65(6); U_{33} 44(6); U_{12} 6(4); [b] U_{22} 73(4); U_{33} 58(4); U_{12} −12(3)

earlier the c axis was doubled compared with the ideal case. To avoid problems with i.a. local least squares minima during the initial refinements, the metal compositions at the positions with similar x and y but different z values (0 and 1/2) were slowly and stepwise allowed to refine, while keeping the compositions and coordinates of the remaining positions fixed. The metal composition was described by using fractional occupancies of the different metal ions, with the sum of their occupancies fixed to unity at each position. Due to similar X-ray scattering powers differentiating between Mn and Fe was not possible, both were treated as Mn in the refinements.

During the initial stages of the structure refinement it became apparent that the Sb content was localized to the M(2) and M(13) positions (Tables 2, 3 and Fig. 3). Thus, the metal content at the M(2) and M(13) metal positions was considered as consisting of a mixture of Sb and Mn, while the content at the remaining metal positions was considered as a mixture of Mn(Fe) and Mg. During the structure refinements some of the occupancy factors became insignificantly low ($< 3\sigma$), indicating that the metal position was occupied by only one

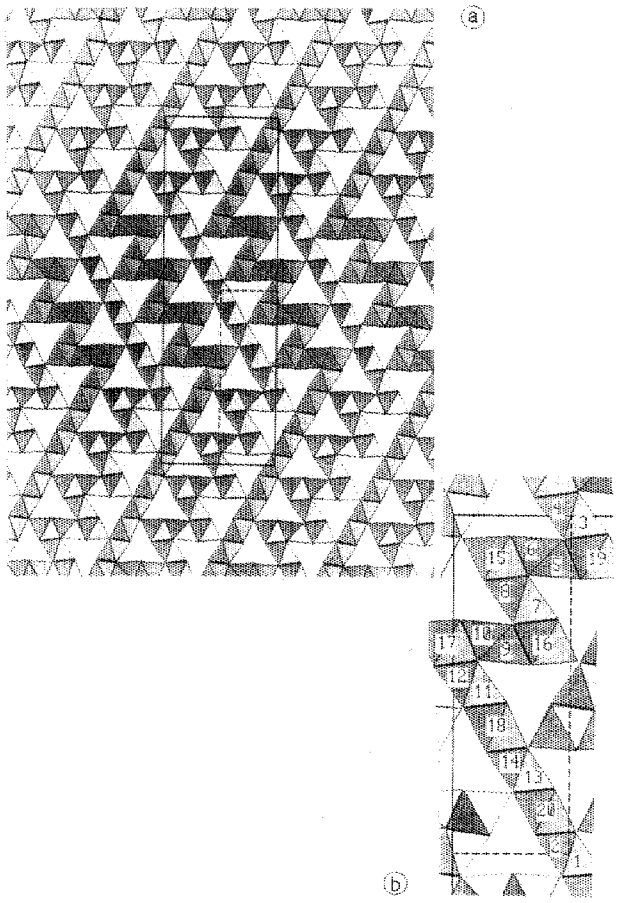

Fig. 3. Polyhedra drawings of the blatterite structure viewed along [001]. For clarity, the trigonal borate groups occupying the triangular channels have been omitted in the drawing. (**a**) The unit cell and the fundamental unit (dashed lines). (**b**) An enlarged picture of the fundamental unit with the atom numbering used for the metal atom positions shown.

Table 3. Metal–oxygen bond distances (with e.s.d.'s) and multiplicities in the coordination octahedra of blatterite. For the disordered metal positions (M(3), M(5) and M(7)), marked with asterisks, the coordinates of the centroids of the octahedra have been used. For the occupancy of the M sites cf. Table 2.

Atoms		Mult.	Distance (Å)
M(1)	O(1)	4	2.122(7)
	O(32)	2	2.149(8)
M(2)	O(1)	4	1.965(7)
	O(31)	2	2.051(9)
M(3)*	O(4)	4	2.268(7)
	O(30)	2	2.255(9)
M(4)	O(4)	4	1.910(7)
	O(29)	2	2.279(9)
M(5)	O(2)	1	2.285(9)
	O(4)	2	2.257(7)
	O(7)	2	2.249(7)
	O(25)	1	2.249(9)
M(6)	O(3)	1	2.300(10)
	O(4)	2	1.908(7)
	O(7)	2	1.916(7)
	O(24)	1	2.244(9)
M(7)*	O(5)	1	2.177(9)
	O(7)	2	2.237(7)
	O(10)	2	2.245(6)
	O(11)	1	2.191(9)
M(8)	O(6)	1	2.260(9)
	O(7)	2	1.942(7)
	O(10)	2	1.925(7)
	O(12)	1	2.336(8)
M(9)	O(8)	1	2.184(9)
	O(10)	2	2.201(7)
	O(13)	2	2.249(7)
	O(14)	1	2.160(9)
M(10)	O(9)	1	2.312(8)
	O(10)	2	1.949(7)
	O(13)	2	1.924(7)
	O(15)	1	2.267(9)
M(11)	O(13)	2	2.306(7)
	O(16)	2	2.054(7)
	O(17)	1	2.193(9)
	O(20)	1	2.148(9)
M(12)	O(13)	2	2.011(7)
	O(16)	2	1.885(7)
	O(18)	1	2.303(9)
	O(19)	1	2.171(8)
M(13)	O(21)	1	2.079(8)
	O(23)	2	1.960(7)
	O(26)	2	1.966(7)
	O(27)	1	2.078(8)
M(14)	O(22)	1	2.097(9)
	O(23)	2	2.111(7)
	O(26)	2	2.122(7)
	O(28)	1	2.193(9)
M(15)	O(1)	1	2.047(7)
	O(2)	1	2.171(9)
	O(3)	1	2.140(10)
	O(5)	1	2.120(9)
	O(6)	1	2.172(9)
	O(7)	1	2.131(7)
M(16)	O(10)	1	2.179(7)
	O(11)	1	2.189(9)
	O(12)	1	2.155(8)
	O(14)	1	2.188(9)
	O(15)	1	2.160(9)
	O(16)	1	1.986(7)
M(17)	O(8)	1	2.194(9)
	O(9)	1	2.118(8)
	O(13)	1	2.141(7)
	O(19)	1	2.168(8)
	O(20)	1	2.097(9)
	O(23)	1	2.022(7)
M(18)	O(16)	1	2.029(7)
	O(17)	1	2.115(9)
	O(18)	1	2.081(9)
	O(21)	1	2.211(9)
	O(22)	1	2.190(9)
	O(23)	1	2.094(7)
M(19)	O(4)	1	2.140(7)
	O(24)	1	2.161(9)
	O(25)	1	2.122(10)
	O(26)	1	2.053(7)
	O(29)	1	2.186(9)
	O(30)	1	2.156(9)
M(20)	O(1)	1	2.039(7)
	O(26)	1	2.043(7)
	O(27)	1	2.167(9)
	O(28)	1	2.077(9)
	O(31)	1	2.213(9)
	O(32)	1	2.074(9)
B(1)	O(5)	1	1.398(16)
	O(8)	1	1.359(16)
	O(28)	1	1.421(16)
B(2)	O(6)	1	1.335(16)
	O(9)	1	1.368(15)
	O(27)	1	1.439(16)
B(3)	O(14)	1	1.361(16)
	O(17)	1	1.403(16)
	O(19)	1	1.400(16)
B(4)	O(15)	1	1.413(16)
	O(18)	1	1.346(16)
	O(20)	1	1.387(16)
B(5)	O(12)	1	1.394(15)
	O(21)	1	1.430(15)
	O(24)	1	1.326(15)
B(6)	O(11)	1	1.405(16)
	O(22)	1	1.347(16)
	O(25)	1	1.412(16)
B(7)	O(3)	1	1.392(16)
	O(29)	1	1.340(16)
	O(31)	1	1.423(16)
B(8)	O(2)	1	1.399(15)
	O(30)	1	1.378(16)
	O(32)	1	1.362(15)

kind of metal ions. This indicated e.g. that M(2) and M(13) was occupied by pure Sb, giving a Sb composition of 0.19 per formula unit in very good agreement with the composition found by the EDX analysis. This supports the conclusion that the only metal positions with any significant Sb content are the M(2) and M(13) positions. Similarly, the metal positions number 4, 6, 8, 10, 11 and 12 were found to be occupied by pure Mn(Fe) and the positions 3 and 20 by pure Mg (Tables 2, 3 and Fig. 3b). No extra conditions were introduced for the positional parameters of any atoms in the final refinements.

The refinements and subsequent $\Delta\varrho$ calculations indicated disordered metal positions at the M(3), M(5) and M(7) positions (Fig. 3b), all belonging to the corrugated C wall. Similar disorder has earlier been observed in other Mn^{3+} containing members of the pinakiolite family (see e.g. Norrestam, Bovin, 1987). To take account of the disorder, the M(3) position was allowed to occupy a fourfold position $(x, y, 0)$ with a fractional occupancy of 0.5, instead of the ideal twofold position $(0, {}^1/_2, 0)$ at the inversion centre. The fourfold M(5) position was split into two fourfold positions M(5a) and M(5b) with occupancies 0.5. To take account of the slight disorder around the M(7) position, occupied by mainly Mn(Fe), two minor satellite positions M(7a) and M(7b) occupied by Mg were introduced. The sum of the occupancies at M(7), M(7a) and M(7b) was kept to unity. Obviously this disorder model can only be regarded as an approximation to the real continuous distribution of the atomic positions in the M(3)—M(5)—M(7) region. To get a picture of the real distribution a $\Delta\varrho$ map, where the contribution to the calculated structure factors from the M(3), M(5) and M(7) metal ions were omitted, is shown in Fig. 4. A further discussion on the origin and nature of this disorder is given below.

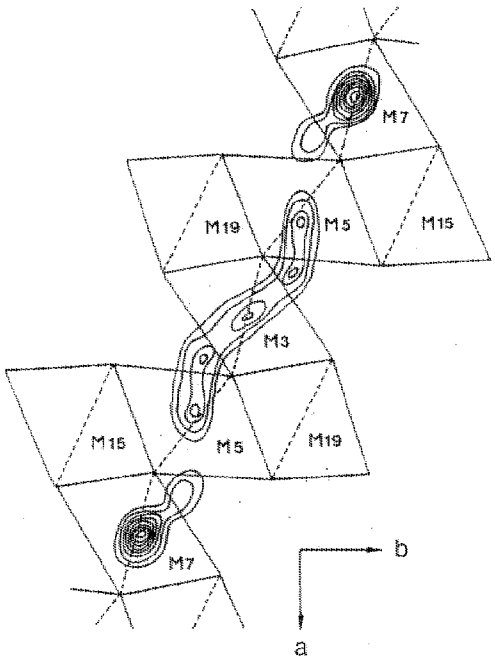

Fig. 4. Difference electron density map ($\Delta\varrho$) in the plane $z = 0$, calculated without the contributions to the structure factors from the various M(3), M(5) and M(7) atomic positions. The oxygen coordination octahedra are outlined. Contours, indicating positive $\Delta\varrho$, are drawn in steps of $3e^-/Å^3$.

Details on the final structure refinement are given in Table 1. The atomic coordinates and occupancies are listed in Table 2.[1] The coordination polyhedra around the metal ions as well as the labelling used for the ions are shown in Fig. 3b. The final structure refinements were carried out by means of the SHELX-76 package (Sheldrick, 1976) slightly modified to run on an IBM PS/2 Model 80 personal computer. The atomic scattering factors used were for neutral atoms and taken from International Tables for X-ray Crystallography (1974). The polyhedral packing diagrams were obtained by means of the computer graphic program POLY (Norrestam, 1984).

Discussion

The oxygen coordination octahedra around the metal ions in the pinakiolite family are linked together by edgesharing to form walls extending in the c direction (Fig. 3a). The walls are linked by cornersharing to other walls and in addition also by the triangular borate groups. The blatterite structure can be derived from that of simple pinakiolite (Fig. 5a) by considering blatterite as consisting of slabs of pinakiolite along the c direction (four unit cells thick) related by glide plane symmetry operations (Takéuchi, 1978). Thus, the flat walls, **F** walls (Fig. 5b), become eleven coordination octahedra wide. The curved walls, **C** walls (Fig. 5c), consisting of the central octahedra through the zig-zag walls become nine octahedra wide (Fig. 3a). The zig-zag walls consist of the **C** walls and of the single **S** columns at the corners of the zig-zag walls (columns of octahedra along the c direction around the metal positions number 15, 16, 17 and 19 in Fig. 3b). The notations **F**, **C** and **S** for the different structure elements of the pinakiolite family were introduced by Takéuchi (1978) and will be used in the description of various structural features below.

The metal positions in the **S** columns are occupied by Mg and Mn, with Mg being a substantial component (49% to 69% Mg). The metal-oxygen bond length distributions do not indicate any appreciable amount of Mn^{3+} at these positions, as no distortion of the coordination octahedra towards a more linear 2 + 4 or planar quadratic 4 + 2 coordination can be distinguished. Thus, the formal metal ion charges at these positions (M(15), M(16), M(17) and M(19)) are probably close to +2.0. Empirical bond valences for the metal ions calculated with the parameter values and the correlation function given by Brown and Altermatt (1985) support such a conclusion, the bond valences are estimated to 2.06, 2.08 and

[1] Additional material to this paper can be ordered referring to the no. CSD 58564, names of the authors and citations of the paper at the Fachinformationszentrum Karlsruhe, Gesellschaft für wissenschaftlich-technische Information mbH, D-76344 Eggenstein-Leopoldshafen, Germany.

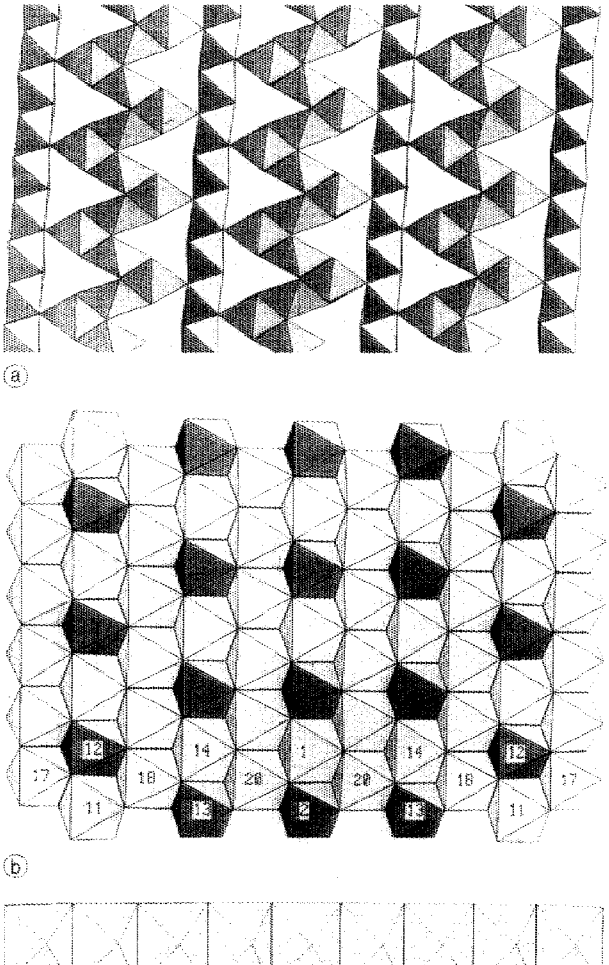

Fig. 5. (**a**) Polyhedral drawing of the monoclinic pinakiolite structure viewed along [010]. The structure, with its characteristic flat (**F** walls) and zig-zag walls (**C** walls) of edgesharing octahedra, is the parent structure of the pinakiolite family. Trigonal borate groups, filling the triangular channels, have been omitted. (**b**) The flat **F** wall of the blatterite structure. The unit translation *c* of 6.200 Å, pointing upwards, corresponds to the size of a pair of edgesharing octahedra. The lighter octahedra are those containing mainly divalent metal ions. (**c**) The **C** wall of the blatterite structure (*c* axis upwards). The row of darker octahedra formed around the M(4), M(6), M(10) and M(12) positions that all contain pure Mn^{3+}, have their sizes successively decreased towards the middle of the wall.

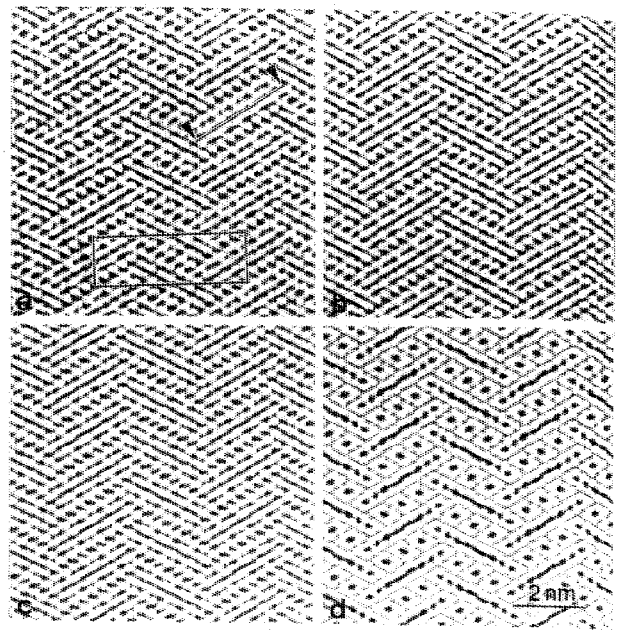

Fig. 6. HREM crystal structure image of a blatterite crystal along [001], recorded with a JEM-4000EX at 400 kV. The unit cell and one scan line along the **C** wall are marked. (**a**) Experimental image. (**b**) Averaged image of Fig. 6a. (**c**) Image symmetrized in accordance with the space group *Pnnm*. (**d**) Computer simulated image, using the coordinates from the X-ray diffraction study.

2.08, respectively. Thus, the **S** columns are formed around metal ions with relatively low formal charge. As was observed also in the corresponding **S** columns of takéuchiite (Norrestam, Bovin, 1987) each of the octahedra have one significantly shorter (about 2.0 Å) metal–oxygen bond and five longer ones (about 2.1 Å). The shorter bonds occur for those oxygen atoms shared between the **S** columns of one zig-zag wall and the **F** wall of another zig-zag wall.

The **F** wall is shown in Fig. 5b together with the labels used for the metal positions. In agreement with earlier observations for members of the pinakiolite family, as pinakiolite, orthopinakiolite and takéuchiite, the metal content in every second **F** wall column (labelled 17, 18 and 20) is dominated (>69% in the present study) by Mg^{2+}. As no typical distortion of the coordination octahedra are observed, the Mn content in the M(17) and M(18) octahedra are likely to be in the form of Mn^{2+} rather than Mn^{3+}. The coordination around the M(20) ion, which is a pure Mg^{2+} position, is distorted and shows four shorter metal–oxygen bonds (2.04 Å to 2.08 Å) and two longer ones (2.17 Å and 2.21 Å). Calculated empirical bond valences agree with the assumption of divalent metal ions at the M(17), M(18), and M(20) positions as they become 2.08, 2.04, and 2.02.

The other three symmetry independent columns forming the **F** wall, contain alternating M(11) + M(12), M(13) + M(14) and M(1) + M(2) positions in each column. Of these, the M(2) and M(13) positions are occupied by pure Sb with coordinations in the form of slightly elongated octahedra with four shorter metal–oxygen bonds of 1.96 Å to 1.97 Å and two longer ones, 2.05 Å to 2.08 Å. The bond distances indicate that the

Sb atoms are pentavalent (Shannon, 1976). This is also supported by a calculation of estimated bond valence estimates yielding the values 5.25 for the M(2) and 5.16 for the M(13) positions. The central column of the wall, consisting of two alternating metal positions, the pure Sb^{5+} position M(2) and the pure Mg^{2+} position M(1) gives an average formal metal ion charge of +3.5. A similar charge is indicated for the column containing the M(13) – M(14) positions as both bond distances and bond valence (2.09) suggest that M(14) is occupied by 40% Mn^{2+} (and 60% Mg^{2+}). In the remaining column of the **F** wall, with the M(11) and M(12) positions, the coordination octahedron around M(12) is substantially distorted towards an elongated octahedron with bond distances typical of Mn^{3+}. The bond valence estimate of 3.00 also support such a conclusion. The coordination around the pure Mn position M(11) is somewhat distorted (two shorter and four longer bonds), but the distances and the estimated bond valence of 2.19 indicate a major divalent Mn content and according the average metal ion charge in this column is about +2.5 (possibly slightly higher).

The structural results indicate that the eleven column wide F walls in blatterite, which is formed by the oxygen coordination around the metal positions 17-(11,12)-18-(13,14)-20-(2,1)-20-(13,14)-18-(11,12)-17 consist of metal ions with average charges 2.0-2.5-2.2-3.5-2.0-3.5-2.0-3.5-2.0-2.5-2.0. Similar charge distributions are found, e.g. in the nine column wide **F** wall of takéuchiite, 2.0-2.5-2.0-3.0-2.0-3.0-2.0-2.5-2.0, in the seven column wide wall of chestermanite (an Sb containing orthopinakiolite, studied by Alfredsson, Bovin, Norrestam and Terasaki, (1991)) 2.0-2.5-2.0-3.5-2.0-2.5-2.0, and in the five column wide wall of magnesium-aluminium ludwigite (Norrestam, Dahl, Bovin, 1988), 2.1-2.6-2.1-2.6-2.1. Apparently, one requirement for obtaining this type of structures with extended flat **F** walls is the presence of different metal ions with charges capable of giving a suitable alternating charge distribution throughout the walls. Evidently, the two end columns of the walls (which also could be interpreted as **S** columns) should have a low metal ion charge. It is then the size of the **F** wall that determines if the central column of the wall should have a higher metal ion charge (as for 3, 7, 11, ... columns) or not (5, 9, ... columns), rather than any structural requirements.

The corrugated nine columns wide **C** wall together with the numbering used for the metal positions are shown in Fig. 5c. In the **C** wall the coordination in every second row (position 4, 6, 8, 10 and 12) is considerable contracted in the *c* direction. This row contains 100% Mn and the bond distance distributions, four shorter coplanar Mn – O bonds of 1.89 Å to 1.95 Å and two longer ones of 2.17 Å to 2.34 Å, as well as estimated bond valences (2.96 to 3.16) clearly indicate all the ions to be trivalent. The two longer bonds in each coordination octahedron extend out of the **C** wall. The octahedra within the rows share edges and as the edgesharing occurs in the plane of the four shorter $Mn^{3+}-O$ bonds, the $Mn^{3+}-Mn^{3+}$ distances in these rows become rather short, 2.71 Å to 2.78 Å.

Except for the **C** walls, the magnitude of the *c* axis is affected by the geometries and sizes of the other structural elements, the **F** walls, the **S** columns and the separation between the borate groups. Thus, the contracted octahedra in the row containing the Mn^{3+} ions will affect the size of the octahedra in the neighboring rows containing the positions number 3, 5, 7, 9 and 11. The octahedra around these positions will become distorted (enlarged) in the *c* direction. From Fig. 5c it is seen, that the distortions increase towards the center of the **C** wall and especially the octahedra around the positions 3, 5 and 7 become very irregular. In view of the short separations, about 2.7 Å, between the centroids along the rows and the extended dimensions of the octahedra perpendicular to the rows, the metal position disorder observed at M(3), M(5) and M(7) seems expectable. Similar types of disorder occur for other Mn^{3+} containing members of the pinakiolite family as in takéuchiite (Norrestam, Bovin, 1987) and in the orthopinakiolite studied by Takéuchi, Haga, Kato and Miura, (1978). On the other hand no such detectable disorder is observed for members without any Mn^{3+} content as in chestermanite, which is of the orthopinakiolite type (Alfredsson et al., 1991) and in magnesium-aluminium ludwigite (Norrestam, Dahl, Bovin, 1988).

As described above, the disorder at the metal positions M(3), M(5) and M(7) was taken care of in the structure refinements by allowing the metal positions to become split up into several subpositions. The disorder model utilized is by necessity an approximation to a real, more continuous disorder, extending over the five octahedra wide region 7-5-3-5-7 of the **C** wall (see also Fig. 5c). The difference electron density map, $\Delta\varrho$, shown in Fig. 4, calculated without the contributions from the split M(3), M(5) and M(7) atoms, also indicates a rather continuous distribution of metal positions in this region. Due to the disorder model used, the 'bond' distances involving the split metal atoms are structurally irrelevant and in Table 3 the distances to the corresponding centroids of the octahedra have been listed instead. It could be noted that estimated bond valences for the centroid positions are low, if the parameter values for Mn^{2+} are used (Brown, Altermatt, 1985) the values for M(3), M(5) and M(7) become 1.67, 1.73 and 1.87, respectively.

The composition of the present blatterite specimen as calculated from the occupancies obtained in the final structure refinement is $Mg_{1.246(7)}Mn_{1.566(7)}Sb_{1.188(1)}O_2BO_3$. This composition agrees well with that found by analysis of the EDX spectra, $Mg_{1.33(2)}Mn_{1.44(2)}Fe_{0.05(1)}Sb_{0.17(1)}O_2BO_3$ (can be written as $Mg_{1.33}(Mn,Fe)_{1.49}Sb_{0.17}O_2BO_3$). The assignments of Mn^{3+} to the metal positions number 4, 6, 8, 10 and 12, Sb^{5+} to positions 2 and 13, and Mn^{2+} or a mixture of Mn^{2+} and Mg^{2+} to the remaining positions give a formal charge of +6.88 for the metal ion content in blatterite ($Mg^{2+}_{1.246}Mn^{2+}_{1.253}Mn^{3+}_{0.313}Sb^{5+}_{0.188}$). This value is close to the charge +7.0 expected for an electroneutral pinakiolite.

Single crystal X-ray diffraction studies give the average structure of the crystal very accurately, while HREM can give important information about the local structure at the atomic level. In order to compare the information from the two methods, experimental HREM images (Fig. 6) were matched against a computer simulated

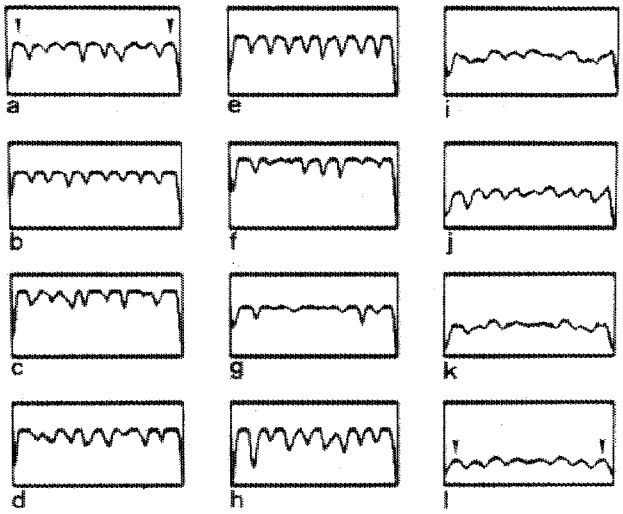

Fig. 7. Graphs of contrast scans along the C walls of Fig. 6. The M(11) and M(12) positions are marked. (**a**–**h**) Scans from Fig. 6a, showing distinct peaks. (**i**–**j**) Scans from Fig. 6b, showing disorder in the middle of the C wall. (**k**) Scans from Fig. 6c, having the space group symmetry. (**l**) Scans from Fig. 6d, for comparison with Fig. 7k.

image calculated with the results from the X-ray study. Some information on the local structure can be obtained by scanning the image contrast (Fig. 7) in the experimental, averaged and simulated images. Most of the scans from the different C walls in the experimental image (Fig. 7a–h) show nine distinct peaks, originating from the metal atom position and indicating that the local structure is ordered. It could be noted from Fig. 4 that the $\Delta\varrho$ map also shows nine peaks, although the shapes and the relative peak heights in $\Delta\varrho$ are different from those of the scanned images. The scans from the averaged (Figs. 7i–j), symmetrized (Fig. 7k) and simulated (Fig. 7l) images, show that the ordering, especially at the three positions in the middle of the C wall, is local and does not extend over more than a few unit cells.

Acknowledgments. Mr. James Anstett is gratefully acknowledged for providing the mineral samples. The availability of the JEM-4000EX and the JSM-840A electron microscopes was made possible through grants from the Alice and Knut Wallenberg Foundation and from the Swedish National Research Council. The Philips EM430 electron microscope was kindly put to our disposal by Prof. Anders Thölén, the Technical University of Denmark. The research program is supported by grants from the Swedish National Energy Administration and the Swedish Natural Science Research Council. The authors are indebted to Mr. Lars Thell for his assistance with the simulation calculations.

References

Alfredsson, V.; Bovin, J.-O.; Norrestam, R.; Terasaki, O.: The structure of the mineral chestermanite, $Mg_{2.25}Al_{0.16}Fe_{0.43}Ti_{0.02}Sb_{0.13}O_2BO_3$. A combined single-crystal X-ray and HREM study. Acta Chem. Scand. **45** (1991) 797–804.

Andersson, S.; Hyde, B.: Twinning on the unit cell level as a structure-building operation in the solid state. J. Solid State Chem. **9** (1974) 92–101.

Bovin, J.-O.; Barry, J.; Thomasson, R.; Norrestam, R.; Fälth, L.: Crystal structure of a new mineral, $(Mg,Mn,Sb)_{2.94}BO_5$. Proc. XIth Int. Congr. on Electron Microscopy, Kyoto 1986. J. Electr. Micr. **S35** (1986) 1697–1698.

Bovin, J.-O.; O'Keeffe, M.; O'Keefe, M. A.: Electron microscopy of oxyborates. I. Defect structures in the minerals pinakiolite, ludwigite, orthopinakiolite and takéuchiite. Acta Crystallogr. **A37** (1981) 28–35.

Brown, I. D.; Altermatt, D.: Bond-valence parameters obtained from a symmetric analysis of the inorganic crystal structure database. Acta Crystallogr. **B41** (1985) 244–247.

Dunn, P. J.; Peacor, D. R.; Simmons, W. B.; Newbury, D.: Frederikssonite, a new member of the pinakiolite group, from Långban, Sweden. Geologiska Föreningens i Stockholm Förhandlingar **105** (1983) 335–340.

International Tables for X-ray Crystallography, Vol. IV, Kynoch Press, Birmingham 1974.

Misell, D. L.: Image analysis, enhancement and interpretation. Elsevier/North-Holland Biomedical Press, Amsterdam 1978.

Norrestam, R.: Computer graphics of polyhedral packing. Acta Crystallogr. S. **A40** (1984) C-438.

Norrestam, R.; Bovin, J.-O.: The crystal structure of takéuchiite, $Mg_{1.71}Mn_{1.29}BO_5$. A combined X-ray and HREM study. Z. Kristallogr. **181** (1987) 135–149.

Norrestam, R.; Dahl, S.; Bovin, J.-O.: The crystal structure of magnesium-aluminium ludwigite, $Mg_{2.31}Al_{0.31}Fe_{0.53}Ti_{0.05}Sb_{0.01}BO_5$. A combined single crystal X-ray and HREM study. Z. Kristallogr. **187** (1989) 201–211.

Norrestam, R.; Hansen, S.: Structural investigation of an antimony-rich pinakiolite, $Mg_{1.90}Mn_{0.91}Sb_{0.19}O_2BO_3$, from Långban, Sweden. Z. Kristallogr. **191** (1990) 105–116.

Norrestam, R.; Nielsen, K.; Søtofte,I.; Thorup, N.: Structural investigation of two synthetic oxyborates: The mixed magnesium-manganese and the pure cobalt ludwigites, $Mg_{1.93}Mn_{1.07}O_2BO_3$ and $Co_3O_2BO_3$. Z. Kristallogr. **189** (1988) 33–41.

Raade, G.; Mladeck, M. H.; Din, V. K.; Criddle, A. J.; Stanley, C. J.: Blatterite, a new Sb-bearing $Mn^{2+}-Mn^{3+}$ member of the pinakiolite group, from Nordmark, N. Jb. Miner. Mh. 3 (1988) 121–136.

Shannon, R. D.: Revised effective ionic radii and systematic studies of interatomic distances in halides and chalcogenides. Acta Crystallogr. **A32** (1976) 751–767.

Sheldrick, G. M.: SHELX-76. Program for crystal structure determination. University of Göttingen 1976.

Stadelmann, P. A.: EMS – a software package for electron diffraction analysis and HREM image simulation in materials science. Ultramicroscopy **21** (1987) 131–146.

Statham, P. J.: Deconvolution and background subtraction by least-squares fitting with prefiltering of spectra. Anal. Chem. **49** (1977) 2149–2156.

Takéuchi, Y.: 'Tropochemical Twinning': A mechanism of building complex structures. Recent Prog. Nat. Sci. Jpn. 3 (1978) 153–181.

Takéuchi, Y.; Haga, N.; Kato, T.; Miura, Y.: Orthopinakiolite, $Me_{2.95}O_2BO_3$: Its structure and relationship to pinakiolite, $Me_{2.90}BO_5$. Can. Mineral. **16** (1978) 475–485.